Design and synthesis of water soluble (metallo)porphyrins with pendant arms: studies of binding to xanthine oxidase†

Elizabeth A. Gibson, Anne-K. Duhme-Klair* and Robin N. Perutz*

Received (in Montpellier, France) 6th December 2009, Accepted 3rd March 2010
First published as an Advance Article on the web 7th April 2010
DOI: 10.1039/b9nj00736a

The tethering of a substrate analogue to a covalently attached luminophore may give rise to a probe for reporting enzyme activity spectrofluorometrically. The overall design incorporates a water-soluble porphyrin luminophore, a substrate analogue and a planar conjugated bridge of the appropriate length designed to bind in the substrate-access channel of xanthine oxidase (XO). 5,10,15-Tris(*N*-methyl-4-pyridiniumyl)-20-phenyl porphyrins was functionalised at the 4-position of the phenyl group with amide-linked 2-methoxy-benzamide groups, [(2-methoxy-4-amino-phenylcarbonyl)-amino] or [(2-methoxy-4-[(pyridine-4-carbonyl)-amino]-phenylcarbonyl)-amino]. The products were isolated as free base or zinc porphyrins with chloride or hexafluorophosphate counterions and characterised by optical emission and absorption in addition to other spectroscopic methods. Binding studies of bovine XO to the zinc porphyrin trichloride derivatives with the above linkers were used to determine the IC_{50} of 81 and 113 μM and K_i values of 4.6 and 6.5 μM, respectively. Furthermore, addition of XO to an aqueous solution of the products caused quenching of the porphyrin emission and a red shift in the absorption spectrum.

Introduction

Photochemical devices, such as 'sensors' or 'probes', are used to transmit information about events occurring on a microscopic or nanoscopic scale *via* light signalling. Ideally they should exhibit high sensitivity, on–off switching, ease of communication and a rapid response. They can be specifically constructed to suit a range of applications and target analytes.[1] Luminescent probes may be designed to be bound within the active site of enzymes by hydrophobic effects and non-covalent interactions.[2] The general principle is to attach a signalling unit (luminophore) covalently to a binding unit *via* a bridge, which will enable communication between the two. Binding of the substrate to the enzyme active site can then be communicated to the signaling unit by energy transfer or electron transfer and the information is reported as a change in the luminescent properties. Each of these distinct components can be specifically designed according to the intended application to maximise supramolecular interactions, tune the spectroscopic properties and redox potentials of the components and to achieve the required water solubility of the molecule.

Both Gray and Lo have combined simplified substrates with covalently attached luminophores giving rise to novel probes for reporting enzyme activity. Examples reported by Lo *et al.* include probes for indole-binding proteins which show protein-induced emission enhancement on binding to tryptophanase and probes for bovine serum albumin, estrogen receptors and biotin conjugates which bind to avidin.[3] Gray and co-workers have developed probes for heme active sites, such as cytochrome $P450_{cam}$ and nitric oxide synthase.[4] The binding is sufficiently strong to allow detection of the enzyme at submicromolar concentrations and is reported by a decrease in emission intensity of the probe luminophore. Both cases demonstrated that changing the length of the linker may simultaneously alter the binding affinity and the rate of energy/electron transfer processes.

Since luminescent probes can be used to study substrate binding and electron transfer reactions of enzymes, we have begun to apply them to another class of clinically significant redox-enzymes, the Xanthine Oxidoreductases (XORs).[5] Xanthine Dehydrogenase (XDH) and Xanthine Oxidase (XO) belong to the multifunctional, multisubstrate Xanthine Oxidoreductase (XOR) family of enzymes.[6,7] These enzymes catalyse the hydroxylation of aromatic heterocycles such as purines, pteridines and aromatic aldehydes (eqn (1)):[5]

$$RH + H_2O \rightarrow ROH + 2H^+ + 2e^- \qquad (1)$$

The oxidation of xanthine to uric acid by the XORs is particularly important in the catabolism of purines, such as ATP.[5,8,9] The reaction occurs at a molybdopterin active site and electrons released are transferred to a second, flavin-containing cofactor.[10] In humans, the enzyme is synthesised as the xanthine dehydrogenase (XDH) form, which uses NAD^+ as the terminal electron acceptor. In the tissues, however, XDH is partially converted to xanthine oxidase (XO), which uses dioxygen as electron acceptor. Consequently, reactive oxygen species, such as hydrogen peroxide as well as superoxide, are produced. XO is therefore a target

Department of Chemistry, The University of York, Heslington, York, YO10 5DD, UK. E-mail: rnp1@york.ac.uk; Tel: +44 (0)1904 432549

† Electronic supplementary information (ESI) available: Dihedral angles and packing diagram of compound **2**, examples of plots used to determine K_i and ^1H and ^{13}C NMR assignments for porphyrins **3–8**. CCDC reference number 757513. For ESI and crystallographic data in CIF or other electronic format see DOI: 10.1039/b9nj00736a

for drugs against oxygen radical-induced tissue damage and oxidative stress, including myocardial reperfusion injury and heart failure.[11] Since a number of medical conditions are associated with XO, there are potential clinical applications for XOR inhibitors which can decrease the activity of the enzyme. A significant number of compounds which bind near the molybdenum cofactor active site have been reported.[10,12] The most potent inhibitors are planar aromatic systems with hydrogen bonding substituents, such as alloxanthine, which are stabilised in the active site by complementary hydrogen bonding residues and π–π-stacking. Drugs can bind tightly in the long, narrow access channel leading to the Mo active site, without directly binding to the molybdenum.[12,13]

The purpose of our substrate analogue attached to the probe is to bind within the access channel to the active site and to communicate with the molybdenum cofactor. The substrate should be bound in the channel by hydrogen bonds and π–π stacking in a similar manner to the natural substrates and so planar heteroaromatic groups are appropriate.[10,14] In addition, direct coordination to the Mo-centre, as observed with the substrate xanthine, may also be possible if suitable donor atoms are introduced, as was demonstrated for the inhibitor Fyx-051 (Scheme 1).[15] Fyx-051 interacts directly with the Mo-centre through a bridging oxygen, which stems from the catalytically active hydroxyl ligand of the Mo-centre. The formation of this intermediate makes Fyx-051 a particularly effective and specific drug candidate.

Attachment and communication between the substrate analogue and luminophore is to occur through a linker of suitable length that positions the substrate close to the molybdenum cofactor in the active site. Computer simulation was used to estimate the length of the linker, although computer simulation from crystal structures can be an over-simplification.[4] Substituents may introduce hydrogen bonding within the molecule, increase rigidity and aid electron transfer. Aromatic groups have been shown to be particularly good bridges.[16] Amide bonds provide a means of connection whilst being able to encourage electron transfer *via* superexchange.[17]

Metalloporphyrins are ideal electron-donating luminophores, which have high extinction coefficients as well as tunable fluorescence emission and redox potentials. Absorption and emission of the chromophore must avoid the region in the spectrum dominated by the cofactors of XO itself (λ_{max} = 280 nm).[5,18] The iron–sulfur clusters of XO contribute absorption maxima at 420 nm, 470 nm and a shoulder at 550 nm and the absorption maxima of the flavin are at 360 and

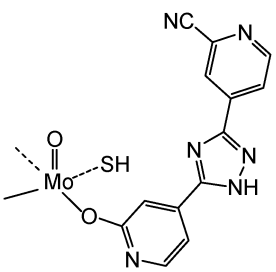

Scheme 1 Proposed interactions between Fyx-051 and the molybdopterin cofactor in XDH according to ref. 15.

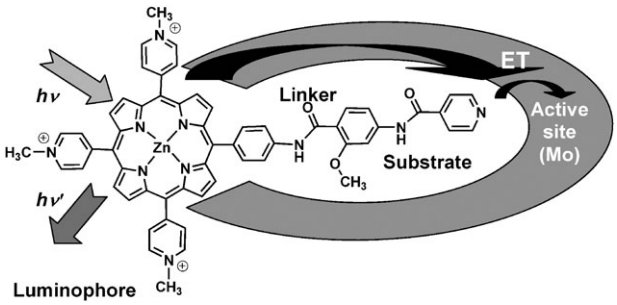

Scheme 2 An example of a probe for XOR. The grey loop represents the active site of XOR.

450 nm. Porphyrins fulfil these requirements and, in addition, can be functionalized at the periphery to suit particular requirements, especially water solubility in biological systems.

We developed our methods by synthesising triphenylporphyrins functionalised by a probe arm consisting of amide-linked 2-methoxy, 4-amino benzamide units.[19] The success of this approach enabled us to move on to water-soluble analogues. Here we report the synthesis and testing of analogous probe molecules based on a water-soluble tris(methylpyridinium) metalloporphyrin with similar pendant arms of different lengths designed to enter the access channel (Scheme 2).

Experimental

General methods

Chemicals came from the following suppliers: triethylamine, ammonium chloride, nicotinic acid (BDH); 4-amino salicylic acid, tetrabutyl ammonium chloride, methyl iodide, nicotinic acid anhydride, isonicotinic acid anhydride, potassium phosphate, Florisil®, xanthine oxidase (bovine milk, grade III, 22 mg ml^{-1}, 1.30 U ml^{-1} as a suspension in 2.3 M $(NH_4)_2SO_4$, 10 mM sodium phosphate buffer, pH 7.8, containing 1 mM EDTA and 1 mM sodium salicylate), Sephadex G-10 (Sigma-Aldrich); allopurinol (Avocado); ammonium hexafluorophosphate (Fluorochem); xanthine (Alfa Aesar); ammonia solution (Fisons); silica gel 60, DMAP (Fluka); NsCl (Lancaster); $[TMPyP][OTs]_4$ kindly donated by Prof. John Lindsay-Smith.

All reactions were carried out under an argon atmosphere unless otherwise stated. All other materials and methods have been described elsewhere.[19]

Synthesis

Methyl 4-amino-2-methoxybenzoate was prepared according to the procedure reported by Hewlett *et al.*[20] Free base 5,10,15-tris(4-pyridyl)-20-(4-aminophenyl)porphyrin was prepared according to the method described by Li *et al.*[21]

Methyl 4-[(pyridine-3-carbonyl)-amino]-2-methoxy benzoate, 1. Triethylamine (0.7 cm^3, 5.0 mmol) was added to a stirred solution of nicotinic acid (0.31 g, 2.5 mmol), DMAP (0.061 g, 0.50 mmol) and NsCl (0.55 g, 2.5 mmol) in acetonitrile (30 cm^3) under argon. The solution was stirred for 20 min at which point a solution of methyl 4-amino-2-methoxybenzoate

(0.50 g, 2.8 mmol) in acetonitrile (10 cm^3) was added at 0 °C. Stirring was continued for 24 h until the reaction was complete by tlc (ethyl acetate). The reaction mixture was concentrated and extracted into 2 M hydrochloric acid. The acidic aqueous phase was washed with ethyl acetate, neutralised with sodium hydrogen carbonate and the resulting precipitate re-extracted into ethyl acetate. The organic fraction was washed with sodium hydrogen carbonate, water and brine and dried over magnesium sulfate. The solvent was removed *in vacuo* to give **1** as a pale yellow powder (0.27 g, 0.94 mmol, 34%); mp 144–146 °C (from ethyl acetate); λ_{max}(DMSO)/nm 284 (ε/dm^3 mol^{-1} cm^{-1} 14 000) and 308 (13 000); ν_{max} (KBr disc)/cm^{-1} 3401w, 3342s, 3199w, 3150w, 3127w, 3090w, 3056w, 3039w, 3012w, 2964w, 2935w, 2913w, 2863w, 2837w, 1687s, 1663s, 1593s, 1532s, 1479w, 1466m, 1448m, 1429m, 1406s, 1341w, 1298s, 1257s, 1202w, 1187w, 1173w, 1147m, 1117w, 1090m, 1026m, 976w, 958w, 886w, 860m, 839w, 827w, 780m, 734w, 704w, 682w, 640w, 620w and 583w; δ_H (300 MHz; $CDCl_3$) 9.11 (1H, s, pyridyl), 8.77 (1H, d, J = 6.0 Hz, pyridyl), 8.33 (1H, s, NH), 8.22 (1H, d, J = 7.3 Hz, pyridyl) 7.85 (1H, d, J = 8.6 Hz, phenyl), 7.72 (1H, d, J = 1.8 Hz, phenyl), 7.44 (1H, dd, J = 4.6, 7.7 Hz, pyridyl), 7.04 (1H, dd, J = 1.7, 8.6, phenyl), 3.91 (3H, s, OCH_3) and 3.87 (3H, s, OCH_3); δ_C (75 MHz; $CDCl_3$) 166.4, 164.5, 160.1, 152.6, 147.9, 143.0, 136.5, 133.4, 130.0, 124.4, 116.1, 111.4, 104.1, 56.5 and 52.4; m/z (ESI^-) 285.0 ($M - H^+$, 100%); m/z (HR ESI^+) 287.1025 ($M + H^+$. $C_{15}H_{15}N_2O_4$ requires 287.1026).

Methyl 4-[(pyridine-4-carbonyl)-amino]-2-methoxy benzoate, 2. The procedure described above was carried out using isonicotinic acid to give **2** as a pale yellow powder (0.30 g, 1.0 mmol, 40%); mp 196–197 °C (from ethyl acetate); δ_H (300 MHz; $CDCl_3$) 8.82 (2H, dd, J = 4.5, 1.6 Hz, pyridyl), 8.04 (1H, s, NH), 7.86 (1H, d, J = 8.5 Hz, phenyl), 7.74 (1H, d, J = 1.8 Hz, phenyl), 7.71 (2H, dd, J = 1.5, 4.4 Hz, pyridyl), 6.99 (1H, dd, J = 1.9, 8.5, phenyl), 3.94 (3H, s, OCH_3) and 3.88 (3H, s, OCH_3); δ_C (75 MHz; $CDCl_3$): 166.3, 164.3, 161.0, 151.3, 142.7, 141.9, 133.4, 121.3, 116.3, 111.3, 104.0, 56.6 and 52.4; m/z (ESI^-) 285.0 ($M - H^+$, 100%); m/z (HR ESI^+) 287.1023 ($M + H^+$. $C_{15}H_{15}N_2O_4$ requires 287.1026).

Free base 5,10,15-tris(4-pyridyl)-20-[4-[(2-methoxy-4-nitro-phenylcarbonyl)-amino]phenyl]porphyrin, 3. Dicyclohexylcarbodiimide (1.40 g, 6.8 mmol) was added to a stirred solution of 2-methoxy-4-nitrobenzoic acid (1.20 g, 6.1 mmol) in acetonitrile (25 cm^3) at 0 °C. After 15 min the reaction was brought to room temperature and stirred for ~24 h until the reaction was complete by tlc (10 : 1 chloroform : acetonitrile v/v). The solution was filtered and the solid by-product was washed thoroughly with acetonitrile and the washings added to the filtrate. Removal of the solvent yielded a pale yellow solid, which was used without any further purification. The anhydride residues were taken up in acetonitrile (20 cm^3) and added dropwise to an ice cold solution of free base 5,10,15-tris(4-pyridyl)-20-(4-aminophenyl)porphyrin (0.64 g, 1.01 mmol) in chloroform with stirring. The reaction was heated at reflux for 48 h. The solvent was removed and the purple residue was extracted into 1 M hydrochloric acid and washed with chloroform (3 × 100 cm^3). The green solution was neutralised with ammonia solution and the resulting purple precipitate was extracted with chloroform. The organic fraction was dried over sodium sulfate and the solution was then concentrated *in vacuo* and the crude product purified by column chromatography (Si-60, 10 : 1 chloroform : methanol v/v) to give **3** (0.71 g, 0.88 mmol, 87%); λ_{max} (DMSO)/nm 422 (ε/dm^3 mol^{-1} cm^{-1} 167 000), 516 (8210), 552 (4140), 590 (2710) and 647 (1790); ν_{max} (KBr disc)/cm^{-1} 3429br m, 3314m, 3077w, 3023w, 2925w, 2854w, 2756w, 2615w, 2536w, 2400w, 2349w, 1716w, 1662m, 1638s, 1589m, 1567w, 1522s, 1480w, 1459m, 1401m, 1383w, 1346m, 1321m, 1279w, 1251m, 1210w, 1182s, 1158w, 1123w, 1085m, 1018m, 999m, 981m, 968s, 897w, 885m, 856m, 801s, 729s, 664w and 639w; δ_H (500 MHz; $CDCl_3$) 10.02 (1H, s, NH), 9.05 (6H, d, *o*-pyridyl), 8.97 (2H, d, β-pyrrole), 8.85 (6H, m, β-pyrrole), 8.58 (1H, d, J = 8.6 Hz, phenyl), 8.23 (2H, d, J = 8.5 Hz, *o*-aminophenyl), 8.17 (6H, d, J = 8.7 Hz *m*-pyridyl), 8.11 (2H, d, J = 8.5 Hz, *m*-aminophenyl), 8.04 (1H, dd, J = 2.0, 8.5 Hz, phenyl), 7.98 (1H, d, J = 2.0 Hz, phenyl), 4.29 (3H, s, OCH_3) and −2.88 (2H, br s, inner NH); δ_C (176 MHz; $CDCl_3$) 161.6, 157.4, 150.8, 150.2, 150.1, 148.3, 138.0, 137.9, 135.3, 134.0, 129.4, 127.3, 121.1, 119.1, 117.5, 117.1, 116.6, 107.1 and 57.3; m/z (ESI^+) 812.3 ($M + H^+$, 100%) and 406.6 ($M + 2H^+$, 15%); m/z (HR ESI^+) 812.2708 ($M + H^+$. $C_{49}H_{34}N_9O_4$ requires 812.2728).

Free base 5,10,15-tris(*N*-methyl-4-pyridiniumyl)-20-[4-[(2-methoxy-4-nitro-phenylcarbonyl)-amino]phenyl]porphyrin tris-(iodide), [4][I]$_3$. Free base **3** (0.067 g, 0.082 mmol) was dissolved in dimethylformide (5 cm^3). Excess methyl iodide (0.1 cm^3) was added and the solution was stirred at room temperature for 12 h. The solvent was removed *in vacuo* to give [**4**][I]$_3$ which was dried in a vacuum oven at 70 °C for 48 h (0.11 g, 0.086 mmol, 96%); λ_{max} (pH 7.5 phosphate buffer)/nm 431 (ε/dm^3 mol^{-1} cm^{-1} 142 000), 524 (12 300), 564 (7710), 592 (6350) and 649 (2630); ν_{max} (KBr disc)/cm^{-1} 3430br m, 3314w, 3077w, 3023br m, 2925br m, 2854w, 2756w, 2615w, 2536w, 2400w, 2349w, 1662m, 1638s, 1589m, 1567w, 1521s, 1479w, 1459m, 1401m, 1383w, 1346m, 1322m, 1279w, 1251m, 1210w, 1182s, 1158w, 1123w, 1083m, 1018m, 999m, 981m, 968s, 897w, 885m, 856m, 801s, 719s, 664m and 639m; δ_H (500 MHz; d_6-DMSO) 10.92 (1H, s, NH), 9.49 (6H, d, *m*-pyridyl), 9.01 (6H, m, *o*-pyridyl), 9.18 (4H, s, β-pyrrole), 9.10 (4H, m, β-pyrrole), 8.25 (4H, m, *o*-, *m*-aminophenyl), 8.03 (2H, m, phenyl), 7.94 (1H, m, phenyl), 4.73 (9H, s, NCH_3), 4.12 (3H, s, OCH_3) and −2.88 (2H, br s, inner NH); δ_C (176 MHz; $CDCl_3$) 164.5, 157.4, 157.1, 157.0, 150.0, 144.7, 139.7, 136.2, 135.4, 132.6, 130.6, 127.6, 123.2, 118.7, 116.2, 115.8, 115.0, 107.5, 57.3 and 48.5; m/z (ESI^+) 856.3 ($M^{3+} + 2e^-$, 25%) and 427.7 ($M^{3+} - H^+$, 15%); m/z (HR ESI^+) 427.6627 ($M^{3+} - H^+$. $C_{52}H_{41}N_9O_4$ requires 427.6635).

Free base 5,10,15-tris(*N*-methyl-4-pyridiniumyl)-20-[4-[(2-methoxy-4-amino-phenylcarbonyl)-amino]phenyl]porphyrin tris-(chloride) [5][Cl]$_3$. Free base [**4**][I]$_3$ (0.100 g, 0.082 mmol) was dissolved in 25 cm^3 ethanol. Saturated ammonium chloride solution (0.1 cm^3) and indium powder (100 mesh, 0.05 g) were added and the solution stirred for 72 h in air, under reflux. The reaction mixture was diluted with water, adjusted to pH 3 with

0.1 M hydrochloric acid and filtered through Celite. The solvent was removed *in vacuo* to give a green/purple solid. The crude porphyrin was taken up in water and ammonium hexafluorophosphate was added to precipitate the product as the hexafluorophosphate salt. This was filtered, washed with cold water and dried to give [**5**][PF_6]$_3$ (0.070 g, 0.055 mmol, 64%).

To obtain the water soluble chloride salt, tetrabutyl ammonium chloride solution in acetonitrile was added dropwise to an acetonitrile solution of [**5**][PF_6]$_3$ to precipitate [**5**][Cl]$_3$. This salt was further purified by passing an aqueous solution through Sephadex G10 size exclusion gel and precipitation from aqueous solution by addition of acetone; λ_{max} (DMSO)/nm 429 (ε/dm^3 mol^{-1} cm^{-1} 124 000), 522 (9780), 564 (8750), 595 (5840) and 653 (3510); ν_{max} (KBr disc)/cm^{-1} 3426br s, 2961w, 2926w, 2855m, 1638s, 1599s, 1590s, 1511s, 1463s, 1400m, 1384s, 1311s, 1271s, 1244s, 1210m, 1182m, 1135m, 1094m, 1052w, 1023s, 1014s, 999m, 981w, 968s, 885w, 821m, 797s, 763m, 729m, 710s and 672m; ν_{max} (ATR)/cm^{-1} 1636s, 1597s, 1588s, 1559m, 1509s, 1468s, 1460s, 1400m, 1359w, 1349w, 1329w, 1312s, 1271s, 1245s, 1211m, 1182s, 1155m, 1136m, 1094m, 1054w, 1024s, 1014s, 998m, 968s, 945w, 927w, 883m, 853s, 793s, 764s, 710s and 663s; δ_H (500 MHz; d_6-DMSO) 10.21 (1H, s, NH), 9.53 (6H, d, *m*-pyridyl), 9.13 (8H, m, β-pyrrole), 9.00 (6H, m, *o*-pyridyl), 8.21 (2H, d, J = 8.2 Hz, *m*-aminophenyl), 8.19 (2H, d, J = 8.2 Hz, *o*-aminophenyl), 7.74 (1H, d, J = 9.0 Hz, phenyl), 6.40 (1H, d, J = 1.9 Hz, phenyl), 6.33 (1H, dd, J = 9.0, 1.9 Hz, phenyl), 4.73 (9H, s, NCH_3), 4.01 (3H, s, OCH_3) and −2.99 (2H, br s, inner NH); δ_C (176 MHz; d_6-DMSO) 164.7, 159.6, 157.1, 157.0, 154.6, 144.7, 140.3, 135.7, 135.4, 133.2, 132.9, 132.6, 123.6, 118.8, 115.8, 114.9, 109.7, 107.0, 96.6, 56.3 and 48.3; m/z (ESI$^+$) 412.7 (M^{3+} − H^+, 15%), 275.5 (M^{3+}, 100%) and 206.8 (M^{3+} + H^+, 10%); m/z (HR ESI$^+$) 275.4526 (M^{3+}. $C_{52}H_{44}N_6O_2$ requires 275.4534).

Free base 5,10,15-tris(*N*-methyl-4-pyridiniumyl)-20-[4-{(2-methoxy-4-[(pyridine-4-carbonyl)-amino]-phenylcarbonyl)-amino}-phenyl]porphyrin tris(chloride), [6][Cl]$_3$. The isonicotinic acid anhydride (0.050 g, 0.18 mmol) was taken up in acetonitrile (50 cm^3) and added dropwise to an ice cold solution of free base [**5**][PF_6]$_3$ (0.068 g, 0.054 mmol) in acetonitrile with stirring. The reaction was heated at reflux for 48 h. Tetrabutylammonium chloride solution in acetonitrile was added dropwise to the cool solution until a precipitate of [**6**][Cl]$_3$ formed. This was filtered, washed with acetonitrile and dried. The product was further purified by passing an aqueous solution through Sephadex G10 size exclusion gel and precipitating from aqueous solution by addition of acetone to give [**6**][Cl]$_3$ (0.043 g, 0.041 mmol, 76%); λ_{max} (pH 7.5 phosphate buffer)/nm 434 (ε/dm^3 mol^{-1} cm^{-1} 117 000), 524 (11 600), 566 (11 800), 598 (8120) and 620 (6520); ν_{max} (KBr disc)/cm^{-1} 3421s, 3109w, 3018w, 2958w, 2917w, 2837w, 1636br s, 1559w, 1539w, 1521m, 1507m, 1475w, 1457w, 1437w, 1401s, 1384s, 1323w, 1260w, 1232w, 1213w, 1182w, 1145w, 1090m, 1072m, 1026s, 964w, 882w, 856w, 794m, 763m, 698m, 668s, 659w and 617w; δ_H (600 MHz; d_6-DMSO) 11.35 (1H, s, NH), 10.58 (1H, s, NH), 9.55 (6H, m, *m*-pyridyl), 9.10 (8H, m, β-pyrrole), 9.01 (8H, m, *o*-pyridyl, *m*-pyridyl), 8.35 (2H, d, J = 5.3 Hz, *o*-pyridyl), 8.29 (2H, d, J = 7.8 Hz, *m*-aminophenyl), 8.23 (2H, d, J = 7.9 Hz, *o*-aminophenyl), 7.95 (1H, s, phenyl), 7.87 (1H, d, J = 8.6 Hz, phenyl), 7.72 (1H, d, J = 8.6, phenyl), 4.75 (9H, s, NCH_3), 4.06 (3H, s, OCH_3) and −2.95 (2H, br s, inner NH); δ_C ([**6**][PF_6]$_3$; 150 MHz; CD_3CN) 164.0, 163.4, 159.4, 158.3, 149.6, 148.3, 144.0, 143.4, 138.7, 138.4, 135.2, 132.8, 132.7, 132.3, 131.6, 123.8, 121.3, 118.7, 118.3, 114.9, 114.0, 112.2, 103.4, 56.3 and 48.4; m/z (ESI$^+$) 465.2 (M^{3+} − H^+, 10%) and 310.5 (M^{3+}, 100%); m/z (HR ESI$^+$) 310.4596 (M^{3+}. $C_{58}H_{47}N_{10}O_3$ requires 310.4605).

Zinc 5,10,15-tris(*N*-methyl-4-pyridiniumyl)-20-[4-[(2-methoxy-4-amino-phenylcarbonyl)-amino]phenyl]porphyrin tris(chloride), [7][Cl]$_3$. Free base [**5**][Cl]$_3$ (0.050 g, 0.054 mmol) and zinc acetate dihydrate (0.11 g, 0.50 mmol) were dissolved in ethanol (25 cm^3) and heated in air, at reflux for 2 h. The reaction mixture was cooled to room temperature and diluted with water (50 cm^3). Ammonium hexafluorophosphate was added to precipitate the product as the hexafluorophosphate salt, [**7**][PF_6]$_3$ (0.058 g, 0.044 mmol, 82%). This was filtered, washed with cold water and dried. To obtain the water soluble chloride salt, tetrabutyl ammonium chloride solution in acetonitrile was added dropwise to an acetonitrile solution of [**7**][PF_6]$_3$ to precipitate [**7**][Cl]$_3$. This product was further purified by passing a methanolic solution of [**7**][Cl]$_3$ through Sephadex LH20 size exclusion gel and precipitation from aqueous solution by addition of acetone to give [**7**][Cl]$_3$ (0.040 g, 0.041 mmol, 76%); λ_{max} (pH 7.5 phosphate buffer)/nm 436 (ε/dm^3 mol^{-1} cm^{-1} 107 000), 565 (11 200) and 615 (6890); ν_{max} (KBr disc)/cm^{-1} 3428br m, 3110w, 3044w, 2963w, 2921m, 2851m, 1636s, 1602s, 1559w, 1518s, 1508s, 1457m, 1400w, 1385m, 1359w, 1341w, 1311w, 1264m, 1241m, 1202w, 1182m, 1129m, 1108w, 1093m, 1016m, 992s, 855w, 797s, 759m, 713m and 673m; δ_H (600 MHz; d_6-DMSO) 10.18 (1H, s, NH), 9.41 (6H, m, *m*-pyridyl), 8.98 (8H, m, β-pyrrole), 8.88 (6H, m, *o*-pyridyl), 8.17 (2H, d, J = 6.0 Hz, *m*-aminophenyl), 8.10 (2H, d, J = 6.0 Hz, *o*-aminophenyl), 7.76 (1H, d, J = 7.5 Hz, phenyl), 6.39 (1H, s, phenyl), 6.32 (1H, d, J = 7.5 Hz, phenyl), 5.95 (2H, br s, NH_2), 4.70 (9H, s, N^+CH_3) and 4.02 (3H, s, OCH_3); δ_C (150 MHz; d_6-DMSO) 164.6, 159.0, 154.6, 150.1, 148.8, 148.6, 148.3, 144.1, 135.0, 133.8, 133.2, 132.6, 132.4, 131.9, 123.8, 115.9, 118.5, 113.9, 109.7, 106.9, 96.6, 56.3 and 48.2; m/z (HR ESI$^+$) 296.0891 (M^{3+}. $C_{52}H_{42}N_9O_2Zn$ requires 296.0912).

Zinc 5,10,15-tris(*N*-methyl-4-pyridiniumyl)-20-[4-{(2-methoxy-4-[(pyridine-4-carbonyl)-amino]-phenylcarbonyl)-amino}phenyl]-porphyrin tris(chloride), [8][Cl]$_3$. Free base [**6**][Cl]$_3$ (0.043 g, 0.041 mmol) and zinc acetate dihydrate (0.075 g, 0.41 mmol) were reacted and converted first to the hexafluorophosphate salt and then the chloride salt as for [**7**][Cl]$_3$, above, to give [**8**][Cl]$_3$ (0.030 g, 0.028 mmol, 67%); λ_{max} (DMSO)/nm 442 (ε/dm^3 mol^{-1} cm^{-1} 111 000), 569 (12 500) and 614 (7520); ν_{max} (KBr disc)/cm^{-1} 3443br w, 3116w, 3043w, 2963w, 2920w, 2849w, 1637s, 1594m, 1526m, 1514w, 1461m, 1453m, 1402m, 1384s, 1342w, 1314m, 1288w, 1262w, 1247w, 1185m, 1129w, 1092m, 1019w, 994s, 853w, 797s, 750w, 715w, 673w and 616w; δ_H (600 MHz; d_6-DMSO) 11.18 (1H, s, NH), 10.98

(1H, s, NH), 9.47 (6H, m, *m*-pyridyl), 9.00 (8H, m, β-pyrrole), 8.92 (6H, m, *o*-pyridyl), 8.81 (2H, d, J = 6.0 Hz, *m*-pyridyl), 8.23 (2H, d, J = 8.2 Hz, *m*-aminophenyl), 8.14 (2H, d, J = 8.2 Hz, *o*-aminophenyl), 7.99 (2H, d, J = 6.0 Hz, *o*-pyridyl), 7.91 (1H, s, phenyl), 7.82 (1H, d, J = 8.2 Hz, phenyl), 7.69 (1H, d, J = 8.2, phenyl), 4.75 (9H, s, NCH_3) and 4.05 (3H, s, OCH_3); δ_C (150 MHz; d_6-DMSO) 164.8, 164.7, 159.0, 157.6, 150.9, 150.8, 148.6, 148.3, 144.1, 142.0, 137.5, 135.0, 133.8, 132.8, 131.8, 131.2, 126.6, 123.7, 122.2, 118.5, 115.9, 115.0, 112.8, 104.4, 55.6 and 48.1; m/z (ESI^+) 496 (M^{2+}, 100%) and 331 (M^{3+}, 80%); m/z (HR ESI^+) 331.0971 (M^{3+}. $C_{58}H_{45}N_1O_3Zn$ requires 331.0984).

Enzyme assay of XO

50 mM potassium phosphate buffer, pH 7.5. Potassium phosphate, monobasic, anhydrous (1.36 g, 10 mmol) was dissolved in deionized water (190 cm^3). A solution of EDTA (0.1 M, 0.2 cm^3) was added and the pH of the solution was adjusted to 7.5 at 25 °C with 1 M potassium hydroxide solution. The volume of the solution was increased to 200 cm^3 with deionized water.

0.15 mM solution of xanthine. Xanthine (2.3 mg, 0.015 mmol) was dissolved in the minimum volume of aqueous potassium hydroxide (1 M). The solution was diluted to 90 cm^3 with deionised water and the pH was adjusted to 7.5 with dilute hydrochloric acid. The solution was made up to 100 cm^3 with deionised water.

Solution of xanthine oxidase. 17 μl of a stock solution of xanthine oxidase (bovine milk, grade III, 22 mg ml^{-1}, 1.30 U ml^{-1}) was diluted to 5 cm^3 with 50 mM potassium phosphate buffer and stored over ice.

Assay procedure

The rate of formation of uric acid was measured spectrophotometrically at 295 nm using the method of Sweeney *et al.* with modifications.[22] All solutions were freshly prepared and stored in an ice bath before use. Enzyme solution (100 μl, 3 mU ml^{-1}) in phosphate buffer (50 mM, pH 7.5) was added to a 2900 μl solution of xanthine and inhibitor in phosphate buffer (50 mM, pH 7.5, 25 °C) giving a final assay concentration of 0.050 mM xanthine (saturated) and 0.1 mU ml^{-1} enzyme. The reaction mixture was stirred and maintained at 25 °C for the duration of the reaction (10 min). A blank was run in the absence of the inhibitor and a control reaction was carried out in the absence of XO. Three replicates were recorded for each inhibitor concentration. The stock solutions of inhibitors that were not water soluble were made up in dimethyl sulfoxide. The final concentration of dimethyl sulfoxide (1%) was not sufficient to affect the assay. In those cases the control reactions were carried out with 1% dimethyl sulfoxide in the final assay.

The IC_{50} was calculated using the sigmoidal fit tool in Origin 6.1 (OriginLab Corporation, Northampton, MA). An example is shown in Fig. S4 in the ESI.†

X-Ray crystallography

Diffraction data were collected on a Bruker Smart Apex diffractometer with MoKα radiation (λ = 0.710 73 Å) using a SMART CCD camera. Diffractometer control, data collection, and initial unit-cell determination were performed using "SMART" (v5.625 Bruker-AXS). Frame integration and unit-cell refinement software was carried out with "SAINT+" (v6.22, Bruker AXS). Absorption corrections were applied using SADABS (v2.03, Sheldrick). The structure was solved by direct methods using SHELXS-97 and refined by full-matrix least squares using SHELXL-97.[23]

Crystal data. $C_{15}H_{14}N_2O_4$, M = 286.28, monoclinic, a = 13.6031(9) Å, b = 8.0726(5) Å, c = 13.6339(9), β = 118.0610(10)°, T = 110(2) K, $P2(1)/n$, Z = 4, reflections measured, 13 200, independent reflections 3270, R_{int} = 0.0194, final R indices [$I > 2\sigma(I)$] R_1 = 0.0364, wR_2 = 0.0979, R indices (all data) R_1 = 0.0403, wR_2 = 0.1011.

Results

Preparation and binding studies of the substrate–linker conjugates

A number of substrate–linker conjugates were prepared so that their affinity for the XO active site could be assessed and the best combination identified for the design of the probe. Commercially available 2-methoxy-4-amino salicylic acid was chosen as the 'linker'. As mentioned above, the enzyme active site accommodates planar aromatic compounds, such as salicylic acid.[10] The acid and amine functionalities provide a means of attachment to the luminophore and substrate by amide coupling. The methoxy group introduces a potential hydrogen bond acceptor which could bind either intramolecularly, to improve rigidity, or intermolecularly to hydrogen bond donor residues lining the access channel of the protein.

Since pyridyl compounds have been shown to be suitable inhibitors, nicotinic and isonicotinic acid were coupled to the linker.[12] The DMAP-catalysed reaction shown in Scheme 3 gave **1** and **2** in 34% and 40% yield, respectively, after recrystallisation from ethyl acetate.[24] The successful amide coupling was indicated by the downfield chemical shift of the NH proton in the ^{1}H NMR spectrum at δ 8.77 for **1** and δ 8.04 for **2**.

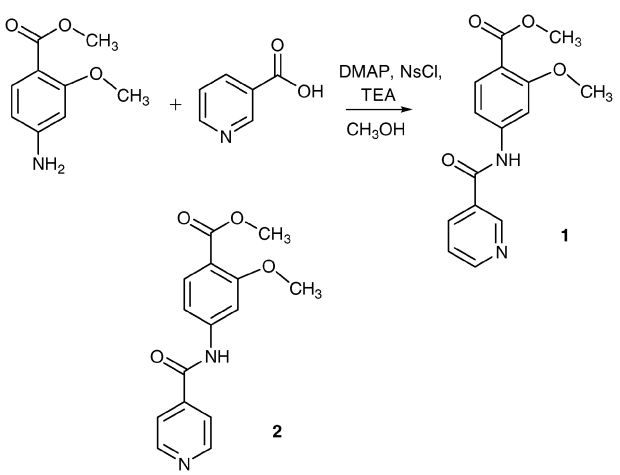

Scheme 3 Preparation of substrate–linker conjugates **1** and **2**.

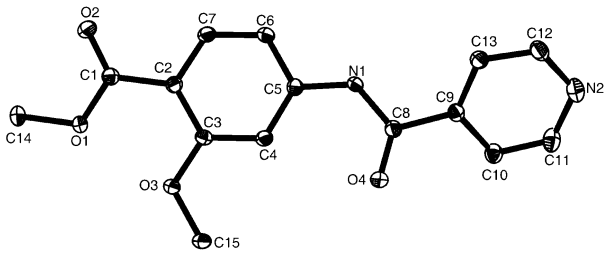

Fig. 1 ORTEP view of **2** with 50% thermal ellipsoids; hydrogen atoms not shown.

Table 1 Selected bond lengths and angles for **2**

Bond	Length/Å	Bond	Angle/°
C(1)–O(2)	1.2153(13)	O(2)–C(1)–C(2)	123.21(9)
C(1)–O(1)	1.3315(12)	O(1)–C(1)–C(2)	115.48(9)
C(1)–C(2)	1.4817(14)	O(3)–C(3)–C(4)	121.89(9)
C(3)–O(3)	1.3583(12)	O(3)–C(3)–C(2)	117.78(9)
C(5)–N(1)	1.4042(13)	O(4)–C(8)–N(1)	124.21(9)
C(8)–O(4)	1.2194(13)	O(4)–C(8)–C(9)	119.97(9)
C(8)–N(1)	1.3627(13)	N(1)–C(8)–C(9)	115.82(9)
C(14)–O(1)	1.4450(12)	C(8)–N(1)–C(5)	127.50(9)
C(15)–O(3)	1.4311(12)		

Compound **1** was a powder that showed little tendency to form crystals from organic solvents, while **2** readily formed large, transparent blocks on slow evaporation of solvent from a concentrated solution in ethyl acetate. The molecular structure was determined by X-ray diffraction (Fig. 1, Table 1). The two aromatic rings in **2** and the amide and ester groups deviate from co-planarity as indicated by the dihedral angles N(1)–C(8)–C(9)–C(13) of 26.72° and O(2)–C(1)–C(2)–C(7) of 12.45°, respectively. The angle between the fitted planes of the two aromatic rings is 29.35 (0.04)° (see ESI† for dihedral angles, Table S1). A possible reason for this twist can be inferred from the packing diagram. A weak hydrogen bond between N(1) of one molecule and the ester carbonyl oxygen, O(2), on another molecule creates a supramolecular array of species (Fig. S1 (ESI†), N(1)–H(1)···O(2)#1 d(N···O) = 2.062(15) Å). The pyridyl nitrogen does not act as a H-bond acceptor, nor is there any π–π-stacking between the aromatic groups.

In order to compare the binding affinity of the compounds prepared, enzyme inhibitor studies were carried out.[22] The percent inhibition is calculated from eqn (1), where v is the initial rate of formation of uric acid monitored at the absorption maximum, 295 nm with inhibitor and v_0 is the initial rate without the inhibitor. The %inhibition was found to vary by ±5% between the three replicate runs. A plot of %inhibition *vs.* log [I], where [I] is the inhibitor concentration, is fitted to a sigmoidal function to yield the IC_{50} (Table 2, estimated experimental error ±10%). Some of the inhibitors were not sufficiently soluble at concentrations that gave close to 100% inhibition. In those cases, the upper limit was fixed at 100%. The UV/vis spectrum of the inhibitors was recorded over time to ensure no degradation reaction was taking place. In order to provide a means of comparison with literature data, the IC_{50} of allopurinol was measured as a control experiment. Since the IC_{50} is dependent on the conditions of the assay, of which there is a great variation across published data, the binding constant, K_i, was calculated from eqn (2).

$$\%\text{inhibition} = 100(1 - v/v_0) \quad (1)$$

$$IC_{50} = (1 + [S]/K_m)K_i \quad (2)$$

where IC_{50} is the concentration of inhibitor required to reduce the rate of the reaction by 50%, [S] is the concentration of the substrate. K_m was estimated using the double-reciprocal plot of $1/v$ *vs.* $1/[S]$ which gives a straight line of gradient K_m/V_{max} and intercept on the $1/v$ axis of $1/V_{max}$ and on the $1/[S]$ axis of $-1/K_m$ (see ESI† for figures). A value of K_m = 3.05 μM was obtained which is consistent with that reported.[25]

Table 2 IC_{50} and K_i values for each of the compounds with XO. (Errors in IC_{50} ± 10%)

Compound	IC_{50}/μM	K_i/μM
Allopurinol	17	0.98
Methyl 4-amino-2-methoxybenzoate	163	9.4
4-Amino-2-methoxybenzoic acid	416	24
Nicotinic acid	946	54
Isonicotinic acid	1270	73
1	179	10
2	130	7.5
[**7**][Cl]$_3$	81	4.6
[**8**][Cl]$_3$	113	6.5

Table 2 lists the IC_{50} and K_i values determined for each of the compounds that were shown to inhibit XO. Both the linker motif and the proposed substrate bound to XO with K_i values in the micromolar range, suggesting that they are suitably accommodated in the XO active site, competing with the binding of xanthine. The compounds with free carboxylic acid groups bound less tightly than the ester equivalents. Since the K_i for the isonicotinic acid-based compound **2** was slightly lower than that of the nicotinic acid isomer, **1**, and structural information was available for **2**, isonicotinic acid was chosen as the substrate analogue for the porphyrin-based probe.

Preparation of the porphyrin derivatives

Our approach to the synthesis of the porphyrin derivatives involved coupling of 5,10,15-tris(4-pyridyl)-20-(4-aminophenyl)-porphyrin, prepared using the method described by Li *et al.*, to 2-methoxy-4-nitrobenzoic acid using the DCC-mediated method described for TPP derivatives (Scheme 4).[21]

Compound **3** was obtained, in 79% yield, using the anhydride procedure previously described.[19] Nitro compound **3** was methylated with methyl iodide as described by Li *et al.*[21] Methylation in all three positions was shown to be complete by ^{1}H NMR spectroscopy and ESI-MS. The iodide salt, [**4**][I]$_3$, was reasonably soluble in water and ethanol. [**4**][I]$_3$ was reduced with indium and ammonium chloride in 64% yield and precipitated as the hexafluorophosphate salt to yield [**5**][PF$_6$]$_3$.[26] The ^{1}H NMR spectrum and ESI-MS indicated that the free base compound, not the indium porphyrin, was present at this stage.[19] Water solubility of the compound could be achieved by conversion to the chloride salt [**5**][Cl]$_3$.

Isonicotinic acid itself was not sufficiently soluble in the solvents appropriate for the DCC-mediated coupling procedure to attach the linker. Therefore commercially available

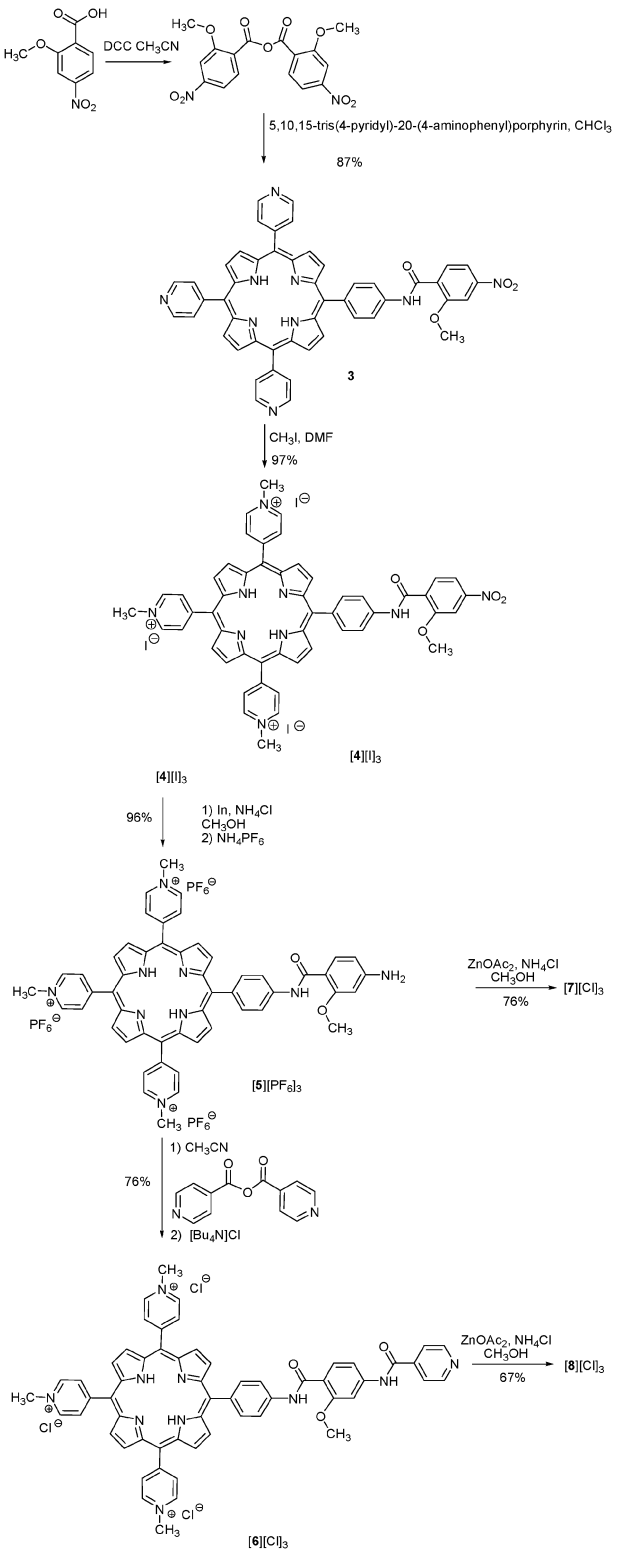

Scheme 4 Synthesis of porphyrin–linker conjugates [**7**][Cl]$_3$ and [**8**][Cl]$_3$.

isonicotinic acid anhydride was used directly and compound [**6**][Cl]$_3$ was prepared in 76% yield after purification.

The porphyrins [**5**][Cl]$_3$ and [**6**][Cl]$_3$ were metallated with $Zn(OAc)_2{\cdot}2H_2O$ following the procedure reported by Miyatani and Amao.[27] The progress of the reaction could be monitored by UV-Vis spectroscopy. The metalloporphyrins were purified by addition of ammonium hexafluorophosphate solution to precipitate [**7**][PF_6]$_3$ and [**8**][PF_6]$_3$. The water soluble derivatives could be obtained once more by adding tetrabutylammonium chloride to a solution of [**7**][PF_6]$_3$ or [**8**][PF_6]$_3$ in acetonitrile yielding the porphyrin–linker conjugate, [**7**][Cl]$_3$, and probe compound, [**8**][Cl]$_3$, respectively.

Characterisation

Porphyrins **3–8** were characterized by 1D ^{1}H and ^{13}C NMR spectroscopy and 2D ^{1}H–^{1}H COSY and ^{1}H–^{13}C HMQC and HMBC experiments. The spectra of the water-soluble porphyrins were recorded in d_6-DMSO, since protic solvents such as D_2O and CD_3OD exchange with the NH protons. Despite broadening of the peaks, the spectra were of higher quality for the chloride salts in d_6-DMSO than the PF_6^- salts in CD_3CN. The assignments are provided in the ESI.†

For free base *meso*-5,10,15-tris(4-pyridyl)-20-(4-acetamidophenyl)porphyrin the amide NH resonance was located at δ 7.74 whereas for compound **3** the resonance corresponding to the amide NH protons was shifted further downfield ($\delta \approx 10$) suggestive of intermolecular hydrogen bonding. In general the signals for compound [**4**]$^{3+}$ were broader than for compound **3** due to the more viscous solvent, d_6-DMSO. The amide NH proton was shifted considerably downfield and the inner protons were shifted considerably upfield relative to those of **3**, possibly due to hydrogen bonding with the solvent.

The ^{1}H NMR spectra of [**6**]$^{3+}$ included additional doublets at δ 8.35 and at δ 9.01 corresponding to the pyridyl protons that were absent in [**5**]$^{3+}$. Two amide signals are located at δ 11.35 and 10.58. The resonance of the NH nearest to the phenyl linker is shifted further downfield due to hydrogen bonding to the neighbouring methoxy compared to that of the NH nearest to the pyridyl substrate for which there is no neighbouring hydrogen bond acceptor. The resonance of the latter is shifted downfield compared to that recorded for compound **2** (δ 8.04) possibly due to hydrogen bonding to the solvent (**2** was recorded in $CDCl_3$).

In the ESI-MS, the M + H$^+$ adduct was observed for **1** and **2** but a different ionisation pathway was observed for **4**. A peak at m/z = 856 corresponding to reduction of the porphyrin, possibly by iodide ($M^{3+} + 2e^-$), was observed. The rest of the porphyrins were already charged and therefore the corresponding M^{3+} ions were observed.

Table 3 Porphyrin Q and Soret (S) absorption maxima (nm) and absorption coefficients ε (10^3 dm^3 mol^{-1} cm^{-1}) in 0.5 mM potassium phosphate buffer, pH 7.5

	S λ_{max} (ε)	Q1 λ_{max} (ε)	Q2 λ_{max} (ε)	Q3 λ_{max} (ε)	Q4 λ_{max} (ε)
3[a]	422 (167)	516 (8.21)	552 (4.14)	590 (2.71)	647 (1.79)
TMPyP	422 (235)	518 (16.3)	554 (6.43)	585 (7.52)	640 (2.00)
[**4**]I_3	431 (142)	524 (12.3)	564 (7.71)	592 (6.35)	649 (2.63)
[**5**]Cl_3	429 (124)	522 (9.78)	564 (8.75)	595 (5.84)	653 (3.51)
[**6**]Cl_3	434 (117)	524 (11.6)	566 (11.8)	598 (8.12)	620 (6.52)
[**7**]Cl_3	436 (108)	565 (10.3)	615 (6.04)		
[**8**]Cl_3	442 (110)	569 (11.5)	614 (6.52)		

[a] **3** in chloroform.

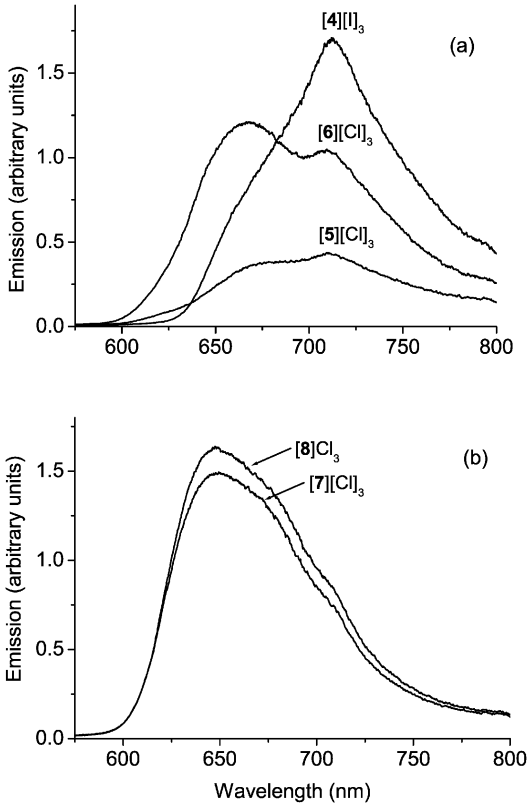

Fig. 2 Corrected and optically matched emission spectra in 50 mM potassium phosphate buffer, pH 7.5: (a) [**4**][I]$_3$, [**6**][Cl]$_3$, λ_{ex} = 420 nm, [**5**][Cl]$_3$; (b) [**7**][Cl]$_3$ and [**8**][Cl]$_3$, λ_{ex} = 435 nm.

Each porphyrin displayed characteristic absorption bands in the visible region with significant variation with the functional groups *i.e.* nitro, amine *vs.* pyridine (Table 3). The extinction coefficients for the zinc porphyrins were lower than those of the free base porphyrins, possibly as a result of coordination to water. The absorption spectra for compounds [**4**]$^{3+}$, [**5**]$^{3+}$ and [**6**]$^{3+}$ were all substantially red-shifted compared to those of **3** and TMPyP. The Soret bands of probes [**7**]$^{3+}$ and [**8**]$^{3+}$ are both red-shifted relative to the corresponding free base compounds, causing their green colour.

Compounds **4–8** dissolved in phosphate buffer each gave broad emission bands between 600 and 800 nm upon excitation at 420 nm. The quantum yields were lower than that of TMPyP but were sufficiently high to compete with the absorption from XO under assay conditions. Fig. 2a shows the emission spectra of free base porphyrins [**4**]$^{3+}$, [**5**]$^{3+}$ and [**6**]$^{3+}$. The emission spectrum of compound [**4**]$^{3+}$ was similar to that of TMPyP in shape and emission maximum; the quantum yield was *ca.* 50% of that of TMPyP. The quantum yields of compounds **5** and **6** were much lower and the spectra contained a more conspicuous shoulder at shorter wavelength. The emission spectra for the zinc porphyrins **7** and **8** (Fig. 2b) are similar with respect to intensity and λ_{max}. The spectra are blue-shifted and more intense relative to those of the free base derivatives.

Effects of XO on the probe absorption and emission spectra

Enzyme affinity bioassays were carried out for probes **7** and **8**. The IC_{50} and K_i for each are listed in Table 2 and Fig. 3 shows

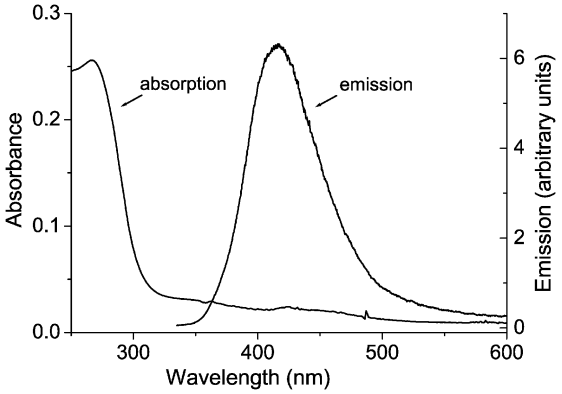

Fig. 3 Absorption spectrum for XO and emission spectrum for XO (λ_{ex} = 325 nm).

the absorption and emission spectra for XO in phosphate buffer (50 mM, pH 7.5). The porphyrin absorption bands occur at longer wavelength than the absorption maximum for the enzyme. Similarly, the emission bands are at longer wavelength for porphyrins **5–8** than that of XO. These properties are essential for an efficient probe.

A solution of XO in phosphate buffer (bovine milk, grade III, 22 mg cm^{-3}, 1.30 U cm^{-3}, 10 μl) was added to each of the water-soluble porphyrins, **5–8**. In each case the absorption decreased by ~30% and a small red-shift (1–3 nm) was observed. Fig. 4a illustrates the spectrum of **5** in the presence of XO. This was matched by a 30% decrease in emission

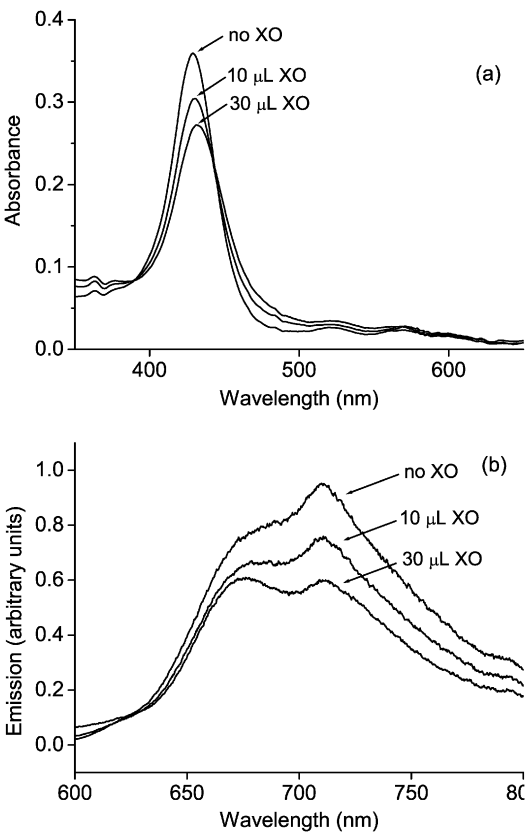

Fig. 4 Effect of adding XO to [**5**][Cl]$_3$ in phosphate buffer pH 7.5; (a) absorption spectra; (b) corrected emission spectra (λ_{ex} = 420 nm).

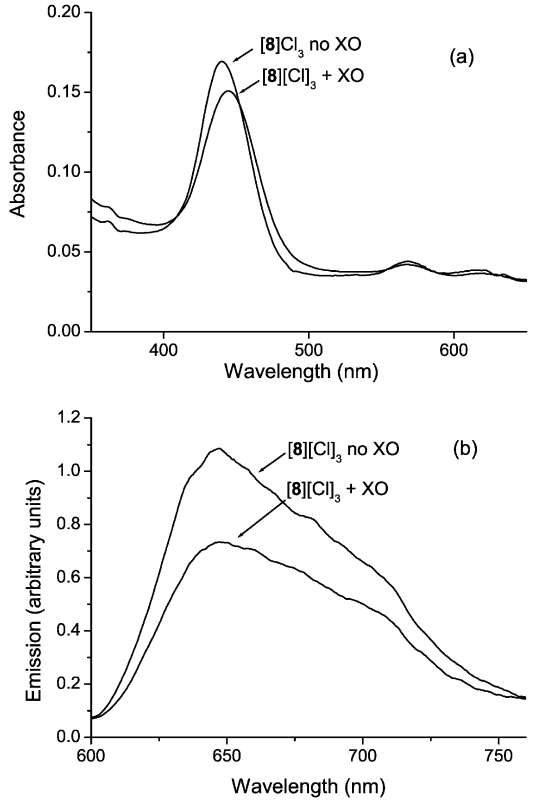

Fig. 5 Effect of adding XO to [**8**][Cl]$_3$ in phosphate buffer pH 7.5; (a) absorption spectra; (b) corrected emission spectra (λ_{ex} = 570 nm).

intensity (Fig. 4b). The absorption spectrum for $[\mathbf{8}]^{3+}$ was also red-shifted on addition of XO (441–446 nm) (Fig. 5a). The relative quantum yields were compared by examining the ratio of the integrated emission intensity (Fig. 5b) per unit of absorbance; the quantum yield was reduced by 25%. These observations show that the porphyrin does report the presence of XO by a change in luminescence and absorption. Addition of allopurinol did not result in restoration of the luminescence. Therefore it has not been conclusively proven that the quenching is due to binding to the active site and not just to the enzyme surface. However, neither of these effects was observed for TMPyP, suggesting that the change is not due to interaction with the enzyme surface alone.

Discussion

Water-soluble zinc porphyrin derived probes, designed to report binding to xanthine oxidase (XO), have been prepared according to Scheme 4. The probes are composed of a porphyrin luminophore, a linker and a substrate analogue. A straightforward strategy was used to couple the aromatic units sequentially, using amide coupling chemistry based on the experiments with triphenyl porphyrins reported previously.[19] The need for amine protecting groups was avoided by using the corresponding nitro compound and selectively reducing the coupled species with indium and ammonium chloride to give the amine. This procedure was suitable for preparing the simple substrate–linker compounds **1** and **2** in addition to neutral and cationic porphyrin–linker compounds **3** and **4** and extended porphyrin–linker–substrate compounds **5–8**.

4-Amino-2-methoxybenzoic acid was chosen as the linker since it contains aromatic rings and possible hydrogen bond donor and acceptor groups. It can therefore interact with residues lining the access channel leading to the active site of the enzyme. The neutral ester derivative, methyl 4-amino-2-methoxybenzoate, was shown to bind to XO with K_i = 9.4 μM. Since the enzyme catalyses the oxidation of aromatic, nitrogen containing heterocycles, pyridine derivatives were also studied. Isonicotinic acid was shown to bind to the enzyme with K_i = 73 μM. However, when coupled to the linker (**2**) the binding was improved to K_i = 7.5 μM, making it a suitable choice as the substrate analogue.

The porphyrin luminophore absorbed strongly in the visible region of the electromagnetic spectrum where there is little competition with absorption of the chromophore of XO. The chloride salts of the pyridinium derivatives were highly water-soluble, which is required for the XO affinity bioassay. There is also a possibility for interaction of the cationic groups with the negatively charged surface areas of the protein.[10] Zinc was incorporated to give an electron donating metalloporphyrin. It was anticipated that photoinduced electron transfer from the metalloporphyrin to the molybdenum cofactor active site on excitation into the probe bands would result in quenching of the luminescence and would therefore signal binding of the probe.

Enzyme affinity bioassays were carried out on the porphyrin compounds to investigate their ability to bind to XO. The IC_{50} for the substrate-analogues and substrate–linker conjugates in xanthine oxidase affinity assays were measured by spectrophotometric rate determinations. The values obtained were used to aid design of [**8**][Cl]$_3$. The K_i for each of the compounds was found to be in the micromolar range (Table 2). The binding affinity for the substrate–linker conjugates was much higher than that for the linker and substrate analogues themselves. K_i for the reference compound, allopurinol, was found to be 0.98 μM, in agreement with the value reported by Ho and Clifford, K_i = 0.91 μM.[28]

The IC_{50} of [**7**][Cl]$_3$ (81.2 μM) was approximately five times that of allopurinol (IC_{50} 17 μM), suggesting that the porphyrin–linker conjugate already has a reasonable affinity for xanthine oxidase. The value was half that of the linker alone, possibly due to improved water-solubility and additional ionic interactions of the cationic porphyrin periphery with the anionic residues around the channel on the enzyme surface.[10] Since compound [**7**][Cl]$_3$ was not displaced by allopurinol, the channel may be blocked by the porphyrin, preventing access. ZnTMPyP did not inhibit XO and, therefore, inhibition by compound [**7**][Cl]$_3$ is likely to be associated with interactions between the enzyme and the probe 'arm', linker and substrate moieties.

For [**7**][Cl]$_3$, the K_i = 4.6 μM is lower than that of [**8**][Cl]$_3$ (K_i = 6.5 μM). The longer probe 'arm' of **8** may affect the binding in the channel in two ways: matching to the depth of the channel and the potential for direct interaction with the molybdenum active site. Nonetheless an IC_{50} in the 100 μM scale is suitable for an application as a probe for XO since it is sufficient to be measured but low enough to allow

displacement by strong inhibitors ($IC_{50} < 1$ μM). The absorption spectrum for the probe, [**8**][Cl]$_3$, was red-shifted in the presence of XO and the quantum yield was 25% lower than in the absence of the enzyme.

Conclusions

The compounds described here have been shown to interact with XO. The porphyrins report interaction with the protein by a change in the absorption and luminescence properties, as anticipated. Compound **8** had a lower affinity for XO (IC_{50} = 113, K_i = 6.5 μM) than compounds **7** and methyl 4-amino-2-methoxybenzoate. Despite its weaker binding to XO, the longer probe 'arm' should approach more closely or bind directly to the active site molybdenum. As a result there is more opportunity for quenching of the luminescence by electron transfer. Indeed, addition of XO to an aqueous solution of [**8**][Cl]$_3$ did cause quenching of the porphyrin emission and a red shift in the absorption spectrum. The K_i is in the low micromolar region which may be suitable for use in screening for XO inhibitors, where the displacement of the probe by active analytes (such as febuxostat, K_i = 20 nM)[29] would restore the porphyrin luminescence provided that the access is not prevented by the porphyrin unit.

The synthetic procedure has been shown to be highly versatile, enabling synthesis of triphenyl porphyrin derivatives as well as water-soluble trimethylpyridiniumyl porphyrins. Further modification of the linker and substrate-analogue, such as substitution of different *N*-heterocycles for isonicotinic acid, should be reasonably straightforward. Likewise, derivatisation around the porphyrin periphery is not restricted to methylation of the pyridyl nitrogens.

At this stage we have successfully designed and synthesized probe molecules that bind to XO. It is not yet proved conclusively that they bind in the substrate access channel. Possible future work includes co-crystallisation of the probes with XO and porphyrin excitation in the presence of indicators that would show the formation of reactive oxygen species such as peroxides and superoxides formed during the reaction where oxygen is the final electron acceptor.

Acknowledgements

EAG is grateful to EPSRC for a studentship. We thank Dr Adrian Whitwood for assistance with the X-ray structure.

Notes and references

1 L. Fabbrizzi and A. Poggi, *Chem. Soc. Rev.*, 1995, **24**, 197; J. F. Callan, A. P. de Silva and D. C. Magria, *Tetrahedron*, 2005, **61**, 8551.
2 E. Meggers, *Chem. Commun.*, 2009, 1001.
3 J. S.-Y. Lau, P.-K. Lee, K. H.-K. Tsang, C. H.-C. Ng, Y.-W. Lam, S.-H. Cheng and K. K. W. Lo, *Inorg. Chem.*, 2009, **48**, 708; K. K. W. Lo, K. H.-K. Tsang, K.-S. Sze, C.-K. Chung, T. K.-M. Lee, K. Y. Zhang, W.-K. Hui, C.-K. Li, J. S.-Y. Lau, D. C.-M. Ng and N. Zhu, *Coord. Chem. Rev.*, 2007, **251**, 2292; K. K. W. Lo, M.-W. Louie, K.-S. Sze and J. S.-Y. Lau, *Inorg. Chem.*, 2008, **47**, 602; K. K. W. Lo, W. K. Hui, C. K. Chung, K. H. K. Tsang, T. K. M. Lee, C. K. Li, J. S. Y. Lau and D. C. M. Ng, *Coord. Chem. Rev.*, 2006, **250**, 1724; K. K. W. Lo and J. S. Y. Lau, *Inorg. Chem.*, 2007, **46**, 700.
4 S. M. Contakes, Y. H. L. Nguyen, H. B. Gray, E. C. Glazer, A.-M. Hays and D. B. Goodin, *Struct. Bonding*, 2007, **123**, 177; Y. H. L. Nguyen, J. R. Winkler and H. B. Gray, *J. Phys. Chem. B*, 2007, **111**, 6628; E. C. Glazer, Y. H. L. Nguyen, H. B. Gray and D. B. Goodin, *Angew. Chem., Int. Ed.*, 2008, **47**, 898; C. A. Whited, W. Belliston-Bittner, A. R. Dunn, J. R. Winkler and H. B. Gray, *J. Inorg. Biochem.*, 2009, **103**, 906; C. Shih, A. K. Museth, M. Abrahamsson, A. M. Blanco-Rodriguez, A. J. Di Bilio, J. Sudhamsu, B. R. Crane, K. L. Ronayne, M. Towrie, A. Vlček Jr., J. H. Richards, J. R. Winkler and H. B. Gray, *Science*, 2008, **320**, 1760.
5 R. Hille, *Chem. Rev.*, 1996, **96**, 2757.
6 J. C. Enroth, B. T. Eger, K. Okamoto, T. Nishino, T. Nishino and E. F. Pai, *Proc. Natl. Acad. Sci. U. S. A.*, 2000, **97**, 10723.
7 T. Nishino, K. Okamoto, Y. Kawaguchi, H. Hori, T. Matsumura, B. T. Eger, E. F. Pai and T. Nishino, *J. Biol. Chem.*, 2005, **280**, 24888.
8 R. Hille and R. F. Anderson, *J. Biol. Chem.*, 2001, **276**, 31193.
9 E.-Y. Choi, A. L. Stockert, S. Leimkühler and R. Hille, *J. Inorg. Biochem.*, 2004, **98**, 841.
10 J. Truglio, K. Theis, S. Leimkühler, R. Rappa, K. V. Rajagopalan and C. Kisker, *Structure*, 2002, **10**, 115; R. Hille, *Arch. Biochem. Biophys.*, 2005, **433**, 107; J. Doonan, A. Stockert, R. Hille and G. N. George, *J. Am. Chem. Soc.*, 2005, **127**, 4518.
11 M. M. Kittleson and J. M. Hare, *Eur. Heart J.*, 2005, **26**, 1458.
12 F. Borges, E. Fernandes and F. Roleira, *Curr. Med. Chem.*, 2002, **9**, 195; Okamoto, B. T. Egers, T. Nishino, S. Kondo, E. F. Pai and T. Nishino, *J. Biol. Chem.*, 2003, **278**, 1848; K. Okamoto, K. Matsumoto, R. Hille, B. T. Eger, E. F. Pai and T. Nishino, *Proc. Natl. Acad. Sci. U. S. A.*, 2004, **101**, 7931; K. Okamoto, A. Fukunari, T. Nishino, B. T. Eger, E. F. Pai, M. Kamezawa, I. Yamada and N. Kato, *J. Pharmacol. Exp. Ther.*, 2004, **311**, 519; T. A. Krenitsky, W. W. Hall, P. de Miranda, L. M. Beauchamp, H. J. Schaeffer and P. D. Whiteman, *Proc. Natl. Acad. Sci. U. S. A.*, 1984, **81**, 3209; T. Sato, N. Ashizawa, T. Iwanaga, H. Nakamura, K. Matsumoto, T. Inoue and O. Nagata, *Bioorg. Med. Chem. Lett.*, 2009, **19**, 184.
13 P. Keith and W. R. Gilliland, *Am. J. Med.*, 2007, **120**, 221.
14 G. Biagi, A. Costantini, L. Costantino, I. Giorgi, O. Livi, P. Pecorari, M. Rinaldi and V. Scartoni, *J. Med. Chem.*, 1996, **39**, 2529.
15 K. Okamoto, K. Matsumoto, R. Hille, B. T. Eger, E. F. Pai and T. Nishino, *Proc. Natl. Acad. Sci. U. S. A.*, 2004, **101**, 7931.
16 K. Kilså, J. Kajanus, A. N. Macpherson, J. Mårtensson and B. Albinsson, *J. Am. Chem. Soc.*, 2001, **123**, 3069; M. U. Winters, K. Pettersson, J. Mårtensson and B. Albinsson, *Chem.–Eur. J.*, 2005, **11**, 562.
17 N. Paddon-Row, *Aust. J. Chem.*, 2003, **56**, 729.
18 V. Massey, P. E. Brumby and H. Komai, *J. Biol. Chem.*, 1969, **244**, 1682.
19 E. A. Gibson, PhD thesis, University of York, 2007.
20 W. A. Hewlett, T. de Paulis, N. S. Mason, D. E. Schmidt, B. L. Trivedi, Z.-J. Zhang and M. H. Ebert, *Chem. Pharm. Bull.*, 1997, **45**, 2079.
21 H. Li, O. S. Fedorova, A. N. Grachev, W. R. Trumble, G. A. Bohach and L. Czuchajowski, *Biochim. Biophys. Acta*, 1997, **1354**, 252.
22 A. P. Sweeney, S. G. Wyllie, R. A. Shalliker and J. L. Markham, *J. Ethnopharmacol.*, 2001, **75**, 273.
23 G. M. Sheldrick, *SHELXS-97, Program for Structure Solution*, University of Göttingen, Göttingen, Germany, 1997; G. M. Sheldrick, *SHELXL-97: Program for the Refinement of Crystal Structures*, University of Göttingen, Göttingen, Germany, 1997.
24 J. C. Lee, Y. H. Cho, H. K. Lee and S. H. Cho, *Synth. Commun.*, 1995, **25**, 2877.
25 J. Escribano, F. Garcia-Canovas and F. Garcia-Carmona, *Biochem. J.*, 1988, **254**, 829.
26 M. R. Pitts, J. R. Harrison and C. J. Moody, *J. Chem. Soc., Perkin Trans. 1*, 2001, 955.
27 R. Miyatani and Y. Amao, *Photochem. Photobiol. Sci.*, 2004, **3**, 681.
28 C. Y. Ho and A. J. Clifford, *J. Nutr.*, 1976, **106**, 1600.
29 N. L. Edwards, *Rheumatology*, 2009, **48**, ii15–ii19.

